APPLICATION OF BIOPHANTOMES TO EVALUATE THE THERMAL EFFECTS OF LASER RADIATION WITH WAVELENGTHS OF 970 NM AND 1560 NM UNDER DIFFERENT EXPOSURE MODES

Ostreiko O.V., Galkin M.A., Papayan G.V., Grishacheva T.G., Petrishchev N.N.
Pavlov First Saint-Petersburg State Medical University, Saint-Petersburg, Russia

Abstract

Laser interstitial hyperthermia is an actively developing direction in intracerebral tumor surgery. The paper presents thermal effects in polyacrylamide biophantoms with bovine albumin and citrated blood under laser irradiation at 970 nm and 1560 nm. For laser irradiation, a surgical two-wave apparatus manufactured by IRE Polis was used. The phantom was irradiated through a quartz optical fiber 400 μm in diameter with an end exit. The result of irradiation of the phantom was its coagulation zone, which was visualized with a FLUM-LL fluorescent organoscope. Thermometry was carried out with a FLIRONE PRO for IOS thermal imager and a T-8 digital thermograph based on a laptop with thermal sensors placed in a phantom. The use of irradiation with a power of not more than 2 W in the coagulation mode, with a total energy dose of up to 120 J, made it possible to achieve a smooth rise in temperature to 88.0 °C. The dimensions of the coagulation zone under irradiation with a wave of 1560 nm were always larger than under irradiation with a wave of 970 nm, although the difference was not statistically significant (p=0,41). Thus, the average coagulation spot area for 970 nm radiation was 43.2 (39.3 – 47.1) mm^2, and for 1560 nm – 99.4 (56.5-141.3) mm^2. With total irradiation with two waves, the coagulation zone was larger if the radiation power of 1560 nm prevailed. When irradiated with a wave of 970 nm, the coagulation zone partially propagates posteriorly from the tip of the optical fiber, and 1560 nm coagulates the phantom anteriorly. The results obtained are of practical importance for laser hyperthermia of intracerebral tumors.

Key words: biophantom, biophantom laser irradiation thermometry, laser hyperthermia of intracerebral tumors, hyperthermia modes.

For citation: Ostreiko O.V., Galkin M.A., Papayan G.V., Grishacheva T.G., Petrishchev N.N. Application of biophantomes to evaluate the thermal effects of laser radiation with wavelengths of 970 nm and 1560 nm under different exposure modes, *Biomedical Photonics*, 2022, vol. 11, no. 2, pp. 12–22.doi: 10.24931/2413–9432–2022–11-2-12-22.

Contacts: Ostreiko O.V., e-mail: oleg.v.ostreiko@mail.ru

ПРИМЕНЕНИЕ БИОФАНТОМОВ ДЛЯ ОЦЕНКИ ТЕРМИЧЕСКИХ ЭФФЕКТОВ ЛАЗЕРНОГО ИЗЛУЧЕНИЯ С ДЛИНАМИ ВОЛН 970 НМ И 1560 НМ ПРИ РАЗНЫХ РЕЖИМАХ ВОЗДЕЙСТВИЯ

О.В. Острейко, М.А. Галкин, Г.В. Папаян, Т.Г. Гришачева, Н.Н. Петрищев
Первый Санкт-Петербургский государственный медицинский университет
им. акад. И.П. Павлова, Санкт-Петербург, Россия

Резюме

Лазерная интерстициальная гипертермия – активно развивающееся направление в хирургии внутримозговых опухолей. В работе представлены термические эффекты в полиакриламидных биофантомах с бычьим альбумином и цитратной кровью при лазерном облучении на длине волны 970 нм и 1560 нм. Для лазерного облучения использован хирургический двухволновый аппарат (ИРЭ «Полис», г. Фрязино, Россия). Облучение фантома осуществлялось через кварцевое световолокно диаметром 400 мкм с торцевым выходом. Результатом облучения была зона коагуляции, которая визуализирована флуоресцентным органоскопом «FLUM-LL». Термометрия осуществлялась тепловизором FLIRONE PRO for IOS и цифровым термографом Т-8 на базе ноутбука с термосенсорами, размещенными в фантоме. Использование облучения мощностью не более 2 Вт в режиме коагуляции с суммарной дозой энергии до 120 Дж позволяло достигать плавного подъема температуры до 88°С. Зона коагуляции при облучении волной 1560 нм всегда

была больше, чем при облучении волной 970 нм, хотя статистически разница была недостоверной (p=0,41). Средняя площадь пятна коагуляции для излучения 970 нм составила 43,2 (39,3 – 47,1) мм^2, для 1560 нм – 99,4 (56,5 – 141,3) мм^2. При суммарном облучении двумя волнами, зона коагуляции была больше, если преобладала мощность излучения 1560 нм. При облучении волной 970 нм зона коагуляция частично распространяется кзади от кончика световолокна, при 1560 нм – коагулирует фантом кпереди. Полученные результаты имеют практическую значимость при применении лазерной гипертермии внутримозговых опухолей.

Ключевые слова: биофантом, термометрия лазерного облучения биофантома, лазерная гипертермия внутримозговых опухолей, режимы гипертермии.

Для цитирования: Острейко О.В., Галкин М.А., Папаян Г.В., Гришачева Т.Г., Петрищев Н.Н. Применение биофантомов для оценки термических эффектов лазерного излучения с длинами волн 970 нм и 1560 нм при разных режимах воздействия // Biomedical Photonics. – 2022. – Т. 11, № 2. – С. 12–22. doi: 10.24931/2413–9432–2022–11-2-12-22.

Контакты: Острейко О.В., e-mail: oleg.v.ostreiko@mail.ru

Introduction

Standard treatments for brain tumors include surgery, radiation therapy, and chemotherapy. Despite an integrated approach to the treatment of malignant glial tumors, the prognosis remains unfavorable. Since surgical treatment is critical, it is necessary to develop effective and less invasive cytoreductive surgical techniques that do not cause damage to healthy tissues. Over the past 30 years, research has been carried out on hyperthermic procedures as an alternative to classical open operations [1–3]. Interstitial hyperthermia of brain tumors under the influence of infrared laser radiation is a less invasive and safer technique than traditional surgical technologies.

Understanding the interaction of laser radiation with tumor tissue and its prediction underlie the development and improvement of laser hyperthermia methods [4]. The wavelength is the fundamental characteristic of laser light, which determines the tissue effects in the irradiated tumor. This is due to the strong dependence of the interaction with the main absorbent molecules in the brain tumor tissue – water and hemoglobin. With this in mind, radiation characteristics are selected, such as power, exposure, power density, and temporal characteristics of radiation. Clinical application of laser thermal destruction in surgery of brain tumors is implemented by the LITT (laser interstitial thermotherapy) method, its purpose is coagulation of tumor tissue controlled by magnetic resonance thermometry [5, 6]. To implement the technology, two Visualase Thermal Therapy System (Medtronic Inc.) and NeuroBlate System (Monteris Medical, Inc.) are currently produced (or commercially available). They use only two wavelengths of laser radiation: 970 nm and 1064 nm, which have similar characteristics of interaction with the tissue, due to the good absorption of these wavelengths by hemoglobin, which provides a hemostatic effect. At The Pavlov First Saint Petersburg State Medical University an original minimally invasive technique for interstitial laser hyperthermia of glial tumors was developed [7]. From a clinical point of view, the use of other wavelengths that have different effects on biological tissue, but are also suitable for interstitial thermal destruction of tumors is of interest.

An important role in the study of thermal effects arising from laser irradiation of biological tissues is played by biophantoms, which have analogous characteristics of thermal conductivity, heat capacity, and heat transfer rate. As close as possible in composition and optical properties to the tissue under study, they allow you to quickly test and visually observe the effects of laser exposure, carried out using different wavelengths in real time. At the same time, despite the absence of microcirculation in biophantoms, it seems possible to study the main characteristics of biological effects (ablation, coagulation, evaporation, carbonization) and the temperature dependence in the hyperthermia zone on the selected wavelength.

To solve research problems, the phantom must contain a pigment that effectively absorbs laser radiation in the required range. As such a pigment, for example, hemoglobin, Chinese ink or Kromagen Magenta MB60-NH concentrate are used. In addition, for the visual assessment of damage caused by the laser, it is important that the phantom is made of transparent material. One way to determine the temperature gradient in a phantom is to introduce thermochromic dyes that change shades depending on the temperature. The introduction of proteins, such as bovine serum albumin (BSA) or hen's egg protein, into the biophantom makes it possible to observe thermal denaturation of the protein, which is noticeable due to clouding of the transparent medium [8-11].

The most popular materials used as the basis for phantoms are agar and polyacrylamide [9, 11, 12]. Polyacrylamide gels are synthesized by the copolymerization of acrylamide and methylenebisacrylamide in an

aqueous solution. Such a gel is transparent and allows visualization and measurement of heat-affected zones. In addition, polyacrylamide itself is a non-toxic, highly stable and biocompatible polymer. For example, N-isopropylacrylamide gel (NIPAM) becomes cloudy when heated to a certain temperature, which can be changed by varying the concentration of acrylic acid. Gels based on NIPAM have acoustic and thermal characteristics close to those of various biological tissues. It is important to note that these gels can be used multiple times. Whereas in a polyacrylamide gel with BSA, thermal treatment leads to irreversible protein denaturation, in the case of NIPAM, the cloudiness caused by heating gradually disappears upon cooling, and the phantom can be used again [13].

The use of phantoms that are as close as possible in terms of the content of chromophores and optical properties makes it possible to conduct test studies, visually observe the effects of laser exposure, measure temperature in real time, describe and predict the propagation of light energy in tissues.

Materials and methods

In the study of the effect of laser radiation on the biophantom, we used two wavelengths: traditional – 970 nm and 1560 nm. Radiation with a wavelength of 970 nm mainly absorbs hemoglobin, 1560 nm – water, including that contained in whole blood (Fig. 1). Such multidirectional interaction with the main chromophores is of practical interest when using laser coagulation of tumors, since it is due to the heterogeneity of the morphological and biological characteristics of neoplasms, including edema, the number of vessels, and cell density in neoplasms of various histological structures and grades of malignancy. In this case, the absorption of laser radiation and the subsequent release of heat in certain areas of the tissue are the key effects in laser hyperthermia of tumors.

When selecting the material for optical phantoms, we took into account both their mechanical properties, such as elasticity, and thermal characteristics. Based on the combination of these properties, the phantom should maximally imitate the studied tissues [15]. We proceeded from the fact that the phantom fabrication procedure should be relatively simple and reproducible. We used a polyacrylamide phantom as the most appropriate type of phantom for modeling the effects of laser exposure on brain tumor tissue. The advantages of such a phantom include transparency, high stability (melting point much higher than 100°C), lack of toxicity, and easy modulation of mechanical properties by changing the concentration of acrylamide/methylenebisacrylamide.

In the manufacture of the phantom, we used data from A.H. Negussie [9, 16], according to which 40% acrylamide/bisacrylamide is mixed with water in a ratio of 1:4.4 (241 ml : 1053 ml). In our study, the ratio corresponded to 1:4.7, which is almost identical. For this phantom, the density corresponds to 1033±1.0 kg/m^3, the thermal conductivity coefficient is 0.590±0.015 W/(m·K), and the thermal diffusivity is 0.145±0.002 mm^2/s. These values are close to those for human soft tissues [17]. According to A. Mohammadi [1], the thermal conductivity index for brain tissue corresponds to 0.563 W/(m·K), thermal diffusivity is 0.147 mm^2/sec.

The phantom was made from the following components:

1. Distilled water. When using laser radiation, there is no need for degassing.

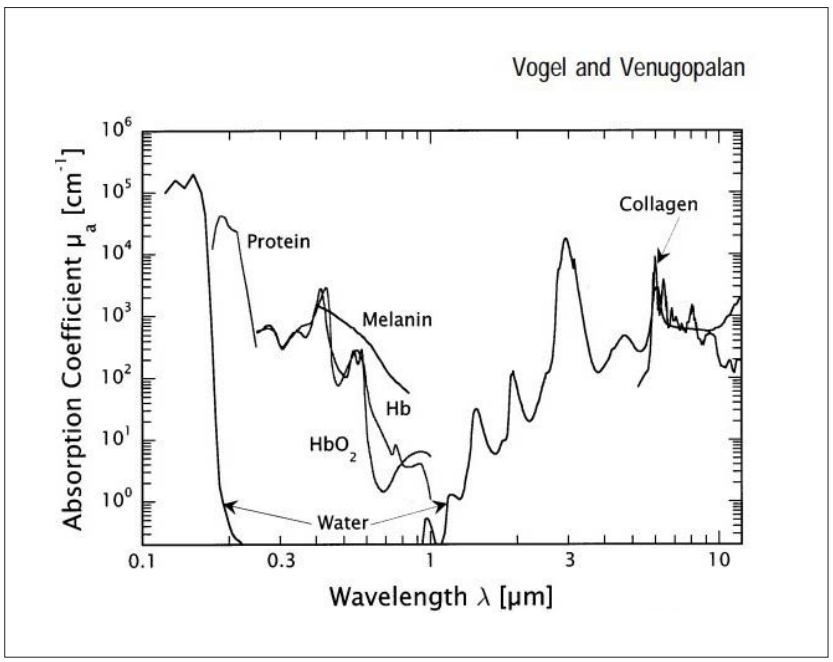

Рис. 1. Коэффициент абсорбции основных тканевых хромофоров для длин волн 100-12000 нм [14] с указанием положения лазерных линий 970 нм и 1560 нм.
Fig. 1. Absorption coefficient of the main tissue chromophores for wavelengths of 100-12000 nm [14] indicating the position of the laser lines 970 nm and 1560 nm.

2. Lyophilised powder of BSA used to detect temperature changes in the phantom and scattering agent. The final concentration of BSA is not less than 5%.

3. Aqueous 40% solution of acrylamide/bisacrylamide, with a weight ratio of acrylamide and bisacrylamide equal to 19:1. The solution is stored at a temperature of 2 to 8°C.

4. Tris/HCl buffer, 1M solution, pH 8.0 (manufacturer – SPD RENAM, Russia).

5. Ammonium persulfate 10% solution for polymerization, prepared ex tempore**.**

6. Hemoglobin (absorbing agent). Citrated blood was used at a ratio of 1 part 3.2% citrate/9 parts whole blood. The formed elements of the blood serve as a scattering agent.

7. TEMED is a polymerizing agent.

8. Sodium azide is a phantom preservative.

To prepare the phantom, we used the following recipe. To 50 ml of distilled degassed water add 5 g of BSA. Stir until complete transition of BSA into solution. Next, 17.5 ml of a 40% acrylamide/bisacrylamide solution, 10 ml of 1M Tris/HCl buffer (pH 8.0) and 600 µl of a 10% ammonium persulfate solution are successively added to the mixture with stirring. Stir until completely homogeneous. Then add citrated blood in an amount depending on the design of the experiment, starting from 750 µl of blood/100 ml phantom. The volume of the mixture is brought to 100 ml with distilled water, then 200 µl of TEMED is added with stirring, the solution is transferred into a round plastic container. Polymerization occurs within 5-10 minutes. In order to prevent dehydration, the resulting gel is stored in a refrigerator in a closed polyethylene container.

To assess the thermal effects, we used a setup that included a two-wave laser apparatus LSP (IRE-Polyus, Fryazino), a miniature thermal imager in the form of an attachment to a smartphone, and a T-8 digital thermograph based on a laptop with thermal sensors. The installation view is schematically shown in Fig. 2.

The phantom was loaded into plastic containers, into which an optical fiber and a thermal sensor were inserted through holes in the side wall (Fig. 3).

The FLIRONE PRO for IOS thermal imager was connected to a smartphone, the display of which displayed a thermal imaging picture with temperature values at selected points, which were recorded in photo and video mode (Fig. 4).

We used a light guide with a direct output of radiation, the modes of which are suitable for use in hyperthermia of brain tumors (Table 1).

Two types of phantom were tested with a lower (F1: 101 mg hemoglobin) and a higher (F2: 202 mg hemoglobin) hemoglobin content. F1 was a model for low- and moderately vascularized tumors, F2 was

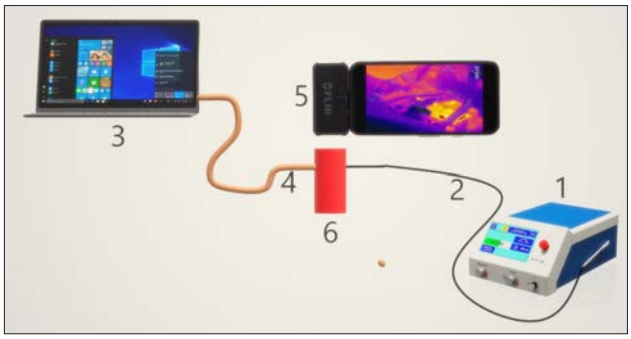

Рис. 2. Установка для изучения влияния лазерного излучения на оптический биофантом: 1 – лазерный аппарат ЛСП («ИРЭ-Полюс», г. Фрязино), 2 – световолокно в держателе, 3 – цифровой термограф Т-8 на базе ноутбука, 4 – термосенсоры, 5 – тепловизионная приставка FLIR ONE PRO for IOS (Китай) вместе со смартфоном iphone 12, 6 – биофантом в контейнере.
Fig. 2. Installation for studying the effect of laser radiation on an optical biophantom. numbers indicate: 1 – laser device LSP ("IRE-Polyus", Fryazino), 2 – optical fiber in the holder, 3 – digital thermograph T-8 based on a laptop with thermal sensors – 4, 5 – thermal imaging attachment FLIR ONE PRO for IOS (China) together with an iphone 12 smartphone, 6 – a biophant in a container.

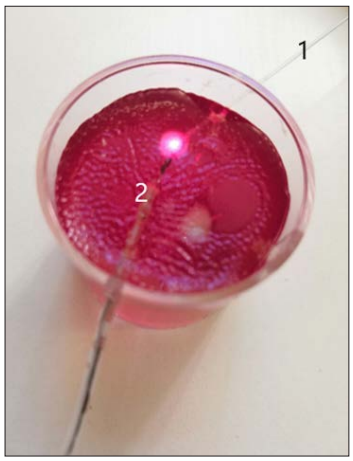

Рис. 3. Внешний вид контейнера с фантомом: в фантом введено световолокно (1), через торец которого наблюдается пилотное лазерное свечение; рядом с торцом установлен термосенсор (2).
Fig. 3. Appearance of the phantom container: an optical fiber (1) is introduced into the phantom, through the end of which a pilot laser glow is observed; a thermosensor (2) is installed near the end face.

Рис. 4. Внешний вид тепловизора FLIRONE PRO for IOS. Стрелка указывает на тепловизор, расположенный как приставка к смартфону над фантомом.
Fig. 4. Appearance of FLIRONE PRO for IOS thermal imager. The arrow points to a thermal imager located as a prefix to a smartphone above the phantom.

Таблица 1
Характеристики используемого лазерного излучения
Table 1
Characteristics of the laser radiation used

Длина волны (нм) Wavelength (nm)	Мощность излучения (Вт) Radiation power (W)	Время облучения (с) Irradiation time (s)	Энергия (Дж) Energy (J)
970	2	60	120
1560	2	60	120
970+1560	2	60	120

a tumor model with a more developed vascular network. The used modes of laser hyperthermia clearly showed heating zones in the form of clouding of the phantom. The size of the clouded zone varied from 4.5 to 5.5 mm (Fig. 5).

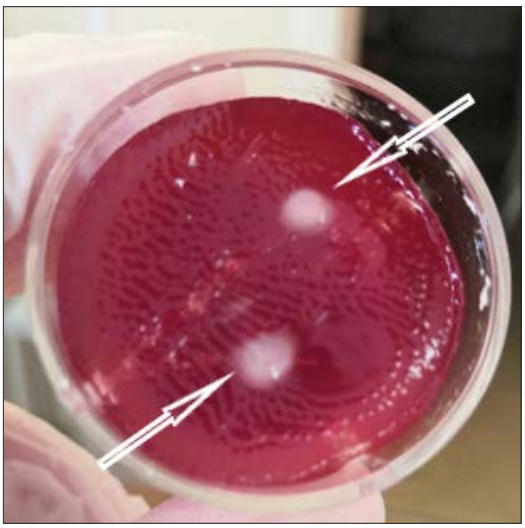

Рис. 5. Фантом. Стрелками показаны зоны помутнения в результате лазерного облучения.
Fig. 5. Phantom. The arrows show the turbidity zones as a result of laser irradiation.

Evaluation of the features of the biophantom coagulation process and the size of the laser coagulation zone at a wavelength of 970 nm and 1560 nm was carried out separately for each of the radiations, or with their combined action. The combined effect of radiation was evaluated under both sequential and simultaneous exposure to the studied wavelengths (Table 2).

Results

The cloudy area of the phantom had an oval-rounded shape. It was noted that in the F2 model, the 970 nm laser radiation creates phantom clouding, propagating anteriorly from the tip of the optical fiber, while the 1560 nm beam was observed to propagate phantom clouding, propagating both forward and posteriorly from the fiber tip. This indicates the difference in both the optical properties of the phantom for different wavelengths and the difference in interaction with chromophores. The combination of two wavelengths in equal proportions demonstrated the dominance of the effects of the 970 nm wavelength, which was also noticed in earlier own studies.

The study of the visual effects of phantom coagulation showed that the maximum area of the coagulation zone when exposed to a wavelength of 1560 nm reached 141.3 mm^2, which is three times more than when exposed to a wavelength of 970 nm (area 47.1 mm^2). The average values of the coagulation spot area were 43.2 (39.3-47.1) mm^2 for 970 nm radiation, and 99.4 (56.5-141.3) mm^2 for 1560 nm radiation (p=0.41). Although the areas of the coagulation spot differed by more than 2 times, the statistical difference was not significant, possibly due to the limited number of experiments. Irradiation with a wavelength of 1560 nm in all cases gave greater heating of the biophantom, which is of great practical importance. Based on the experimental data obtained, further exposure was used with a power of not more than 2 W, with a total energy dose not exceeding 120 J.

The results of laser exposure to the biophantom were visualized in real time using a FLUM-LL fluorescent organoscope [18], which provides multispectral image recording separately in RGB channels in photo and video modes with a resolution of 1280x1024 and a frame rate of 14 Hz (Sony). Although the spectral range of this system is formally limited by a wavelength of 1000 nm, the high brightness of laser radiation made it possible to record a pattern created not only by a 970 nm laser, but also by a 1560 nm laser. The image scale was controlled using a plastic stationery ruler installed directly on the phantom at the time of shooting (Figs. 6 and 7).

From the point of view of the practical use of these wavelengths in the surgery of glial brain tumors,

Таблица 2
Результаты облучения биофантома лазерным излучением с длиной волны 970 нм и 1560 нм
Table 2
Results of irradiation of the biophantom with laser radiation with wavelengths of 970 nm and 1560 nm

Длина волны (нм) Wave length (nm)	Мощность (Вт) Power (W)	Экспозиция (с) Exposure (s)	Энергия (Дж) Energy (J)	Зона коагуляции (мм) Coagulation zone (mm)	Площадь пятна (мм²) Spot area (mm²)	Эффекты коагуляции Effects of coagulation
Облучение одной длиной волны Single wavelength irradiation						
970	2	60	120	5x3	47,1	помутнение фантома clouding of the phantom
1560	2	60	120	9x5	141,3	помутнение фантома clouding of the phantom
Одномоментное облучение двумя длинами волн Simultaneous irradiation with two wavelengths						
970 560	2 2 суммарно total 4	60	240	10x4	125,6	отчетливо слышны щелчки в зоне помутнения фантома clearly audible clicks in the phantom clouding zone
970 1560	1,5 0,5 суммарно total 2	60	120	5x2,5	39,3	помутнение фантома clouding of the phantom
970 1560	0,5 1,5 суммарно total 2	60	120	6x3	56,5	немного слабых щелчков в зоне помутнения фантома a few weak clicks in the phantom clouding zone
970 1560	0,5 2,5 суммарно total 3	60	150	8x4	100,5	немного слабых щелчков в зоне помутнения фантома a few weak clicks in the phantom clouding zone
Последовательное облучение биофантома Sequential biophantome irradiation						
1560 970	2 2	60 60	120 120	7x3	65,9	-
970 1560	2 2	60 60	120 120	7x4 8x5 (повтор)	87,9 125,6	помутнение фантома clouding of the phantom

an important factor was a smoothly and uniformly progressing increase in the area of clouding of the round-oval phantom due to protein coagulation. We did not observe boiling, phantom evaporation, gas bubbles, or smoke. When the phantom was heated, there were no noises, clicks, crackles, etc. This fact indicates the optimal performance of laser radiation for a smooth increase in temperature to 82.8°C from the point of view of safety for the use in brain tumor surgery.

Thermometry

The measurement and distribution of temperature in the phantom as a result of laser irradiation was carried out both using a thermal sensor located near the tip of the optical fiber and using a thermal imaging attachment

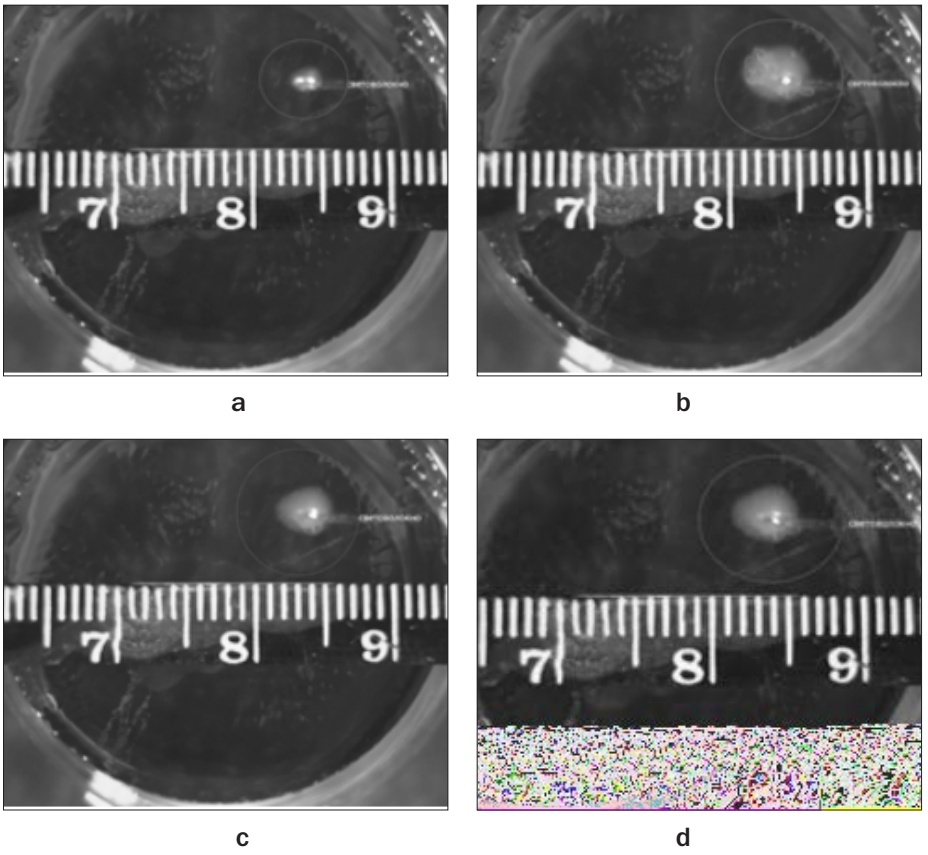

Рис. 6. Визуализация развивающейся зоны коагуляции (выделено кружком) при воздействии на участок фантома лазерным излучением 1560 нм:
a – на 5 с облучения; b – на 20 с;
c – на 40 с; d – на 60 с.
Fig. 6. Visualization of the developing coagulation zone (highlighted by a circle) when the phantom site is exposed to 1560 nm laser radiation:
a – for 5 s of radiation; b – for 20 s;
c – for 40 s; d – for 60 s.

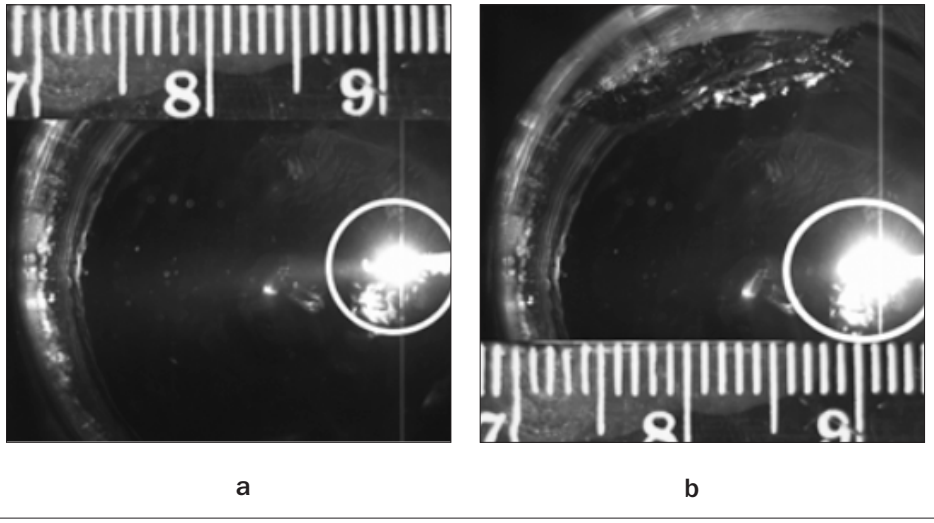

Рис. 7. Распределение лазерного излучения 970 нм в фантоме: a – 5 с воздействия; b – 60 с воздействия.
Fig. 7. Distribution of 970 nm laser radiation in the phantom: a – 5th s of exposure; b – 60th s of exposure.

for a FLIRONE PRO for IOS smartphone, fixed above the phantom (see Fig. 4). The thermal imaging attachment made it possible to estimate the temperature distribution in various parts of the phantom by registering the radiation pattern of the object in the infrared region. Thus, it was possible to simultaneously record the temperature in real time both with the help of a thermal sensor fixed at a distance of 3 mm from the end of the light guide and at three points of the thermal image selected at a distance of about 2 mm from one another. An example of a thermal image of the temperature distribution and the results of its evaluation at 3 points near the end of the optical fiber at the end of 60 s of laser irradiation is shown in Fig. 8. The temperature equal to 82.8°C in the center of irradiation indicated coagulation in this zone. Such a temperature gradient from the fiber tip correlates with *ex vivo* thermometry literature data [19].

Dynamic measurements of the temperature of the F1 phantom at the tip of the optical fiber using a digital thermograph, performed in a constant irradiation mode at a wavelength of 1560 nm, established a relatively rapid increase in temperature in the first 10 s. After 20 s, the temperature changed slightly, averaging 71.8°C (Fig. 9).

When the F1 phantom (with a lower hemoglobin concentration) was irradiated with a laser with a wavelength of 970 nm, a less dynamic and lower heating temperature of the phantom was obtained. In 60 s, it gradually increased from room temperature to 50°C (Fig. 10).

When the phantom was irradiated with a combination of 1560 nm and 970 nm wavelengths with a total power of 2 W, a gradual rise in temperature was also observed, resembling the course of the curve for the 970 nm wave, but reaching a higher level (88°C) with some decrease after 50 s of irradiation. The average temperature during irradiation was 66.9°C (Fig. 11).

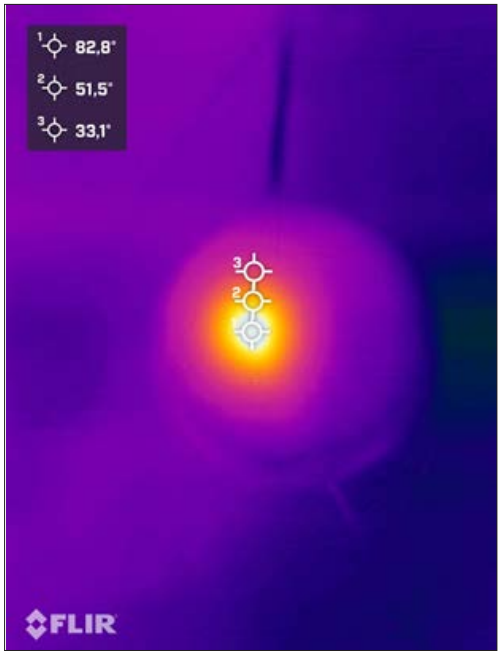

Рис. 8. Тепловизионное изображение участка фантома. Параметры температуры в 3 точках фантома на 60 с облучения длиной волны 1560 нм: 82,8°С у кончика световолокна; 51,5°С на расстоянии 2 мм и 33,1°С на расстоянии 4 мм от кончика световолокна.
Fig. 8. Thermal imaging of the phantom site. Temperature parameters in 3 points of the phantom on the 60th with exposure to a wavelength of 1560 nm: 82.8°C at the tip of the fiber; 51.5°C at a distance of 2 mm and 33.1°C at a distance of 4 mm from the tip of the fiber.

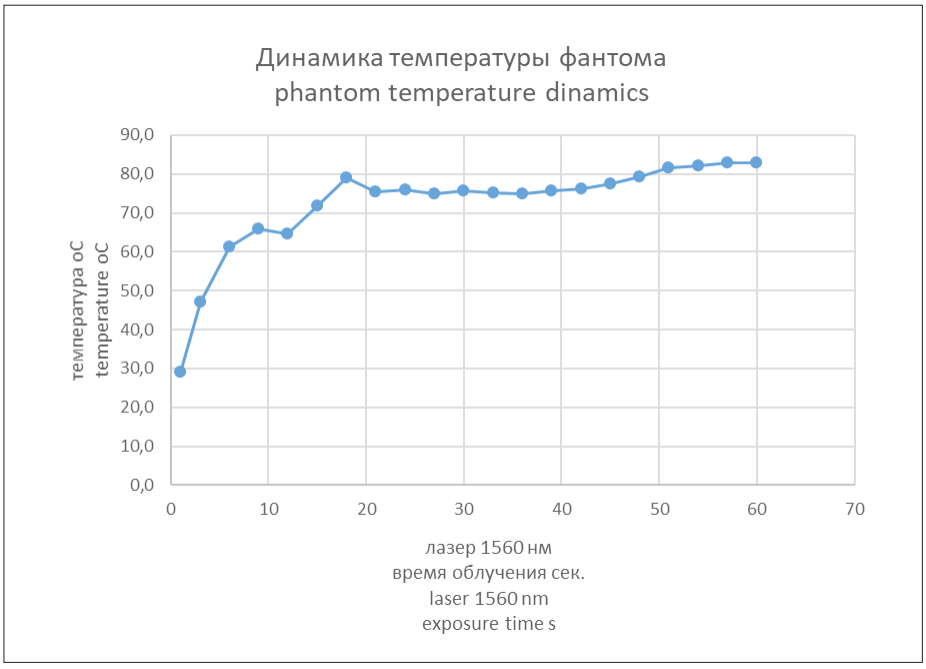

Рис. 9. Динамика температуры фантома при лазерном облучении на длине волны 1560 нм, мощность 2 Вт.
Fig. 9. The temperature dynamics of the phantom under irradiation with a 1560 nm laser, 2 W power.

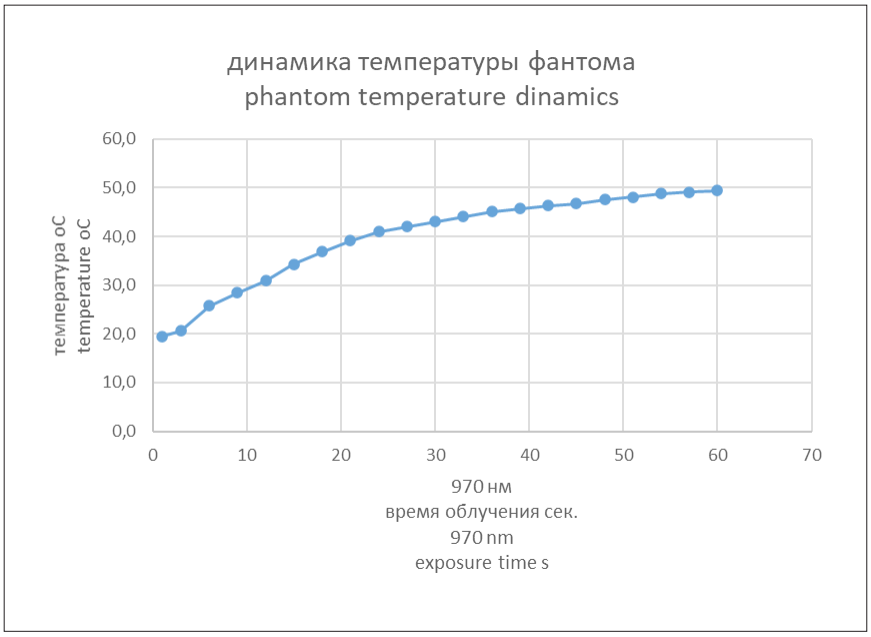

Рис. 10. Динамика температуры фантома при лазерном облучении на длине волны 970 нм, мощность 2 Вт.
Fig. 10. The temperature dynamics of the phantom under irradiation with a 970 nm laser, 2 W power.

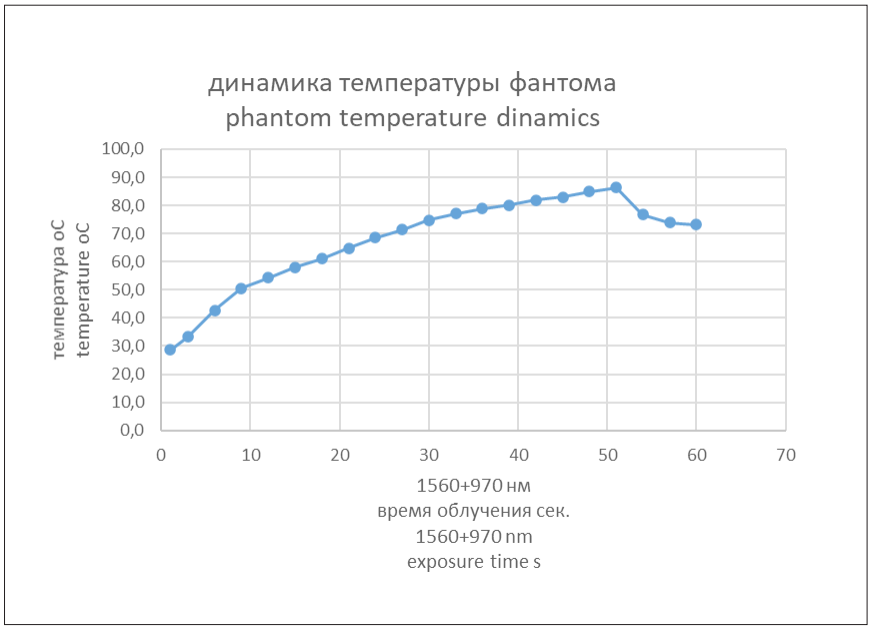

Рис. 11. Динамика температуры фантома у кончика световолокна, при синхронном облучении лазером волнами длиной 1560 нм и 970 нм.
Fig. 11. The temperature dynamics of the phantom at the tip of the optical fiber, during synchronous irradiation with a laser of 1560 nm and 970 nm.

The uneven heating of the phantom observed during irradiation at a wavelength of 1560 nm or a combination of radiation with a wavelength of 970 nm and 1560 nm can be explained by a phase transition of the second type of substance due to heating [20].

Discussion

Thus, the real-time video recording of the process of laser irradiation by the camera visually demonstrated the process of phantom hyperthermia as a brain tumor model. The smoothness of heating, the safe achievement of the coagulation temperatures of the modes used and the dose of laser radiation have been confirmed. The absence of phantom boiling, gas and smoke formation indicates that the temperature in the zone of interaction between the phantom and the laser beam is less than 100°C, which is supported in the methodology of hyperthermia of brain tumors. This fact

was also confirmed by us in an experiment with direct temperature measurement by thermosensors and a thermal imager. This study showed differences in the use of radiation at two wavelengths in temperature effects, sizes of coagulation zones, features of the distribution of the coagulation zone in relation to the tip of the optical fiber. We observed all these effects with the F1 phantom containing a lower concentration of hemoglobin and used as a model of a weakly or moderately vascularized tumor. The F2 phantom with a high hemoglobin content showed coagulation only immediately near the tip of the optical fiber. These features of the interaction should be taken into account when planning the operation, well visualizing areas of the tumor with hypervascularization.

Both methods of temperature measurement demonstrated its smooth rise during irradiation. The farther from the tip of the optical fiber was the thermocouple probe or the temperature measurement point of the thermal imager, the lower the temperature. The difference between temperature measurements by a thermocouple and a thermal imager reached 7°C. This insignificant measurement error by two different methods can be explained by the fact that the thermocouple measures the temperature inside the phantom, while the thermal imager measures the temperature from its surface [21]. Therefore, when fixing the temperature with a thermal imager, we placed the optical fiber at a depth of 1 mm from the phantom surface.

The work was performed on two types of phantoms differing in hemoglobin concentration. This choice was made due to the fact that we consider it important to separate the effects of laser exposure on tumors with different degrees of vascularization, which is due to differences in the level of hemoglobin in tumors. Differences in blood supply require a differentiated approach to the practical application of the laser hyperthermia methodology. Methods for fixing the temperature in a phantom during laser irradiation have been developed and tested. Based on the temperature indicators, it was found that when using real operating modes, the temperature does not exceed 83°C, does not reach the boiling point, the evaporation of the phantom. This confirms the delicacy and safety of these regimens in achieving tumor coagulation. Despite the fact that, in contrast to a tumor, there is no microcirculation in the phantom, this work made it possible to reveal differences in the interaction with the phantom of the two wavelengths used. The obtained results confirm the correctness of the chosen modes of interstitial laser irradiation in minimally invasive hyperthermia of intracerebral tumors.

Conclusion

The heating zone at 1560 nm is always larger than at 970 nm irradiation. Using an irradiation power of more than 2 W, on the one hand, increases the coagulation zone, but audible clicks appear, which indicates ablation of the phantom, boiling due to an increase in temperature above 100°C. Therefore, exceeding the power of interstitial laser radiation by more than 2 W is inappropriate, since it may be associated with undesirable effects in the tumor tissue and the surrounding brain tissue and its vessels. With total irradiation with two waves, the coagulation zone is the larger, the greater the radiation power of 1560 nm. The result of coagulation during sequential irradiation of the biophantom depends little on the sequence of the chosen wavelength. It should be taken into account that when irradiated with a wave of 970 nm, the coagulation zone partially propagates posterior to the tip of the optical fiber; at a length of 1560 nm, almost the entire coagulation zone occurs anterior to the fiber tip. This indicates differences in the interaction and in the optical properties of these two wavelengths with respect to the phantom. The 970 nm radiation propagates less forward, showing smaller penetration in the phantom. The spread of coagulation posteriorly from the tip of the optical fiber is a consequence of the predominance of the reflection of light or the movement of thermal energy posteriorly. All these differences in the distribution of the coagulation zone and temperature dynamics are important to take into account both when planning treatment and in the practical application of the technology of minimally invasive hyperthermia of intracerebral tumors.

REFERENCES

1. Mohammadi A., Bianchi L., Asadi S., Saccomandi P. Measurement of Ex Vivo Liver, Brain and Pancreas Thermal Properties as Function of Temperature. *Sensors (Basel)*, 2021, vol. 21(12), pp. 4236. doi: 10.3390/s21124236
2. Ahmed M., Brace C.L., Fred T Lee Jr. F.T., Goldberg S.N. Principles of and advances in percutaneous ablation. *Radiology*, 2011, vol. 258(2), pp. 351-69. doi: 10.1148/radiol.10081634
3. Franzini A., Moosa S., Servello D., Small I., DiMeco F., Xu Z., Elias W.J., Franzini A., Prada F. Ablative brain surgery: an overview. *Int. J. Hyperth.*, 2019, vol. 36, pp. 64–80. doi: 10.1080/02656736.2019.1616833
4. Geoghegan R., Ter Haar G., Nightingale K., Marks L., Natarajan S. Methods of monitoring thermal ablation of soft tissue tumors - A

ЛИТЕРАТУРА

1. Mohammadi A., Bianchi L., Asadi S., Saccomandi P. Measurement of Ex Vivo Liver, Brain and Pancreas Thermal Properties as Function of Temperature // Sensors (Basel). – 2021. – Vol. 21(12). – P. 4236. doi: 10.3390/s21124236
2. Ahmed M., Brace C.L., Fred T Lee Jr. F.T., Goldberg S.N. Principles of and advances in percutaneous ablation // Radiology. – 2011. – Vol. 258(2). – P. 351-69. doi: 10.1148/radiol.10081634
3. Franzini A., Moosa S., Servello D., Small I., DiMeco F., Xu Z., Elias W.J., Franzini A., Prada F. Ablative brain surgery: an overview // Int. J. Hyperth. – 2019. – Vol. 36. – P. 64–80. doi:10.1080/02656736.2019.1616833
4. Geoghegan R., Ter Haar G., Nightingale K., Marks L., Natarajan S. Methods of monitoring thermal ablation of soft tissue tumors - A

comprehensive review. *Med. Phys.*, 2022, vol. 49(2), pp.769-791. doi: 10.1002/mp.15439
5. Chen C., Lee I., Tatsui C., Elder T., Sloan A.E. Laser interstitial thermotherapy (LITT) for the treatment of tumors of the brain and spine: a brief review. *J. of Neuro-Oncology*, 2021, vol. 151, pp. 429–442. doi: 10.1007/s11060-020-03652-z
6. Lagman C., Chung L.K., Pelargos P.E., Ung N., Bui T.T., Lee S.J., Voth B.L., Yang I. Laser neurosurgery: A systematic analysis of magnetic resonance-guided laser interstitial thermal therapies. *J. Clin. Neurosci.*, 2017, vol. 36, pp. 20-26. doi: 10.1016/j.jocn.2016.10.019
7. Ostreyko O.V., Mozhaev S.V. Way of treatment of glial tumors of a brain of supratentorialny localization. Patent of the Russian Federation for invention No. 2533032 of 16.09.2014.
8. Eranki A., Mikhaila A.S., Negussiea A.H., Prateek S.K., Wooda B.J., Partanen A. Tissue-mimicking thermochromic phantom for characterization of HIFU devices and applications, *International Journal of Hyperthermia*, 2019, vol. 36(1), pp. 518-529. doi: 10.1080/02656736.2019.1605458
9. Negussie A.H., Partanen A., Mikhail A.S., Xu S., Abi-Jaoudeh N., Maruvada S., Wood B.J. Thermochromic tissue-mimicking phantom for optimisation of thermal tumour ablation. *Int. J. Hyperthermia*, 2016, vol. 32(3), pp. 239-43. doi: 10.3109/02656736.2016.1145745
10. Dabbagh A., Jeet Abdullah B.J., Abu Kasim N.H., Ramasindarum C. Reusable heat-sensitive phantom for precise estimation of thermal profile in hyperthermia application. *Int. J. Hyperthermia*, 2014, vol. 30(1), pp. 66-74. doi: 10.3109/02656736.2013.854930
11. Bazrafshan B., Hubner F., Farshid P., Larson M.C., Vogel V., Mantele W., Vogl T.J. A liver-mimicking MRI phantom for thermal ablation experiments. *Med. Phys.*, 2011, vol. 38, pp. 2674–84. doi: 10.1118/1.3570577
12. Davidson S.R.H., Sherar M.D. Measurement of the thermal conductivity of polyacrylamide tissue-equivalent material. *Int. J. Hyperthermia*, 2003, vol. 19(5), pp. 551-62. doi: 10.1080/0265673031000160799 5
13. Ningrum E.O., Purwanto A., Rosita G.C., Bagus A. The Properties of Thermosensitive Zwitterionic Sulfobetaine NIPAM-co-DMAAPS Polymer and the Hydrogels: The Effects of Monomer Concentration on the Transition Temperature and Its Correlation with the Adsorption Behavior. *Indones. J. Chem.*, 2020, vol. 20 (2), pp. 324-335. doi: 10.22146/ijc.41499
14. Vogel A., Venugopoplan V. Mechanisms of Pulsed Laser Ablation of Biological Tissues. *Chem. Rev.*, 2003, vol. 103, pp. 577–644. doi:10.1021/cr030683b
15. Minton J.A., Iravani A., Yousefi A. Improving the homogeneity of tissue-mimicking cryogel phantoms for medical imaging, *Med. Phys.*, 2012, vol. 39(11), pp. 6796-807. doi: 10.1118/1.4757617
16. Guntur S.R., Choi M.J. An improved tissue-mimicking polyacrylamide hydrogel phantom for visualizing thermal lesions with high-intensity focused ultrasound. *Ultrasound in med. and biol.*, 2014, vol. 40(11), pp. 2680-2691. doi: 10.1016/j.ultrasmedbio.2014.06.010
17. Welch A.J., Gemert M.J.C. Optical-thermal response of laser-irradiation tissue. *Springer*, 2011, 947 p. https://doi:10.1007/978-90-481-8831-4
18. Kang U.K., Papayan G.V., Berezin I.B., Jin Bae-Soo, Kim S.V., Petrishchev N.N. Multispectral fluorescent organoscopes for in vivo studies of laboratory animals and their organs. *Optical Journal*, 2011, vol. 78(9), pp. 82-90. (in Russ.). OCIS codes: 170.0170, 170.3880, 170.3890, 170.4580
19. Korganbayev S., Orrico A., Bianchi L., De Landro M., Wolf A., Dostovalov A., Saccomandi P. Closed-Loop Temperature Control Based on Fiber Bragg Grating Sensors for Laser Ablation of Hepatic Tissue. *Sensors 2020*, vol. 20(22), 6496. doi: 10.3390/s20226496
20. Manns F., Milne P.J, Gonzalez-Cirre X., Denham, D.B, Parel J., Robinson D.S. In situ temperature measurements with thermocouple probes during laser Interstitial thermotherapy (LITT): quantification and correction of a measurement artifact. *Lasers Surg. Med.*, 1998, vol. 23(2), pp. 94–103. doi: 10.1002/(sici)1096-9101(1998)23:2<94::aid-lsm7>3.0.co;2-q

comprehensive review // Med. Phys. – 2022. – Vol. 49(2). – P. 769-791. doi: 10.1002/mp.15439
5. Chen C., Lee I., Tatsui C., Elder T., Sloan A.E. Laser interstitial thermotherapy (LITT) for the treatment of tumors of the brain and spine: a brief review // J. of Neuro-Oncology. – 2021. – Vol. 151. – P. 429–442. doi: 10.1007/s11060-020-03652-z
6. Lagman C., Chung L.K., Pelargos P.E., Ung N., Bui T.T., Lee S.J., Voth B.L., Yang I. Laser neurosurgery: A systematic analysis of magnetic resonance-guided laser interstitial thermal therapies // J. Clin. Neurosci. – 2017. – Vol. 36. – P. 20-26. doi: 10.1016/j.jocn.2016.10.019
7. Острейко О.В., Можаев С.В. Способ лечения глиальных опухолей головного мозга супратенториальной локализации // Патент РФ на изобретение №2533032 от 16.09.2014.
8. Eranki A., Mikhaila A.S., Negussiea A.H., Prateek S.K., Wooda B.J., Partanen A. Tissue-mimicking thermochromic phantom for characterization of HIFU devices and applications // International Journal of Hyperthermia. – 2019. – Vol. 36(1). – P. 518-529. doi: 10.1080/02656736.2019.1605458
9. Negussie A.H., Partanen A., Mikhail A.S., Xu S., Abi-Jaoudeh N., Maruvada S., Wood B.J. Thermochromic tissue-mimicking phantom for optimisation of thermal tumour ablation // Int. J. Hyperthermia. – 2016. – Vol. 32(3). – P. 239-43. doi: 10.3109/02656736.2016.1145745
10. Dabbagh A., Jeet Abdullah B.J., Abu Kasim N.H., Ramasindarum C. Reusable heat-sensitive phantom for precise estimation of thermal profile in hyperthermia application // Int. J. Hyperthermia. – 2014. – Vol. 30(1). – P. 66-74. doi: 10.3109/02656736.2013.854930
11. Bazrafshan B., Hubner F., Farshid P., Larson M.C., Vogel V., Mantele W., Vogl T.J. A liver-mimicking MRI phantom for thermal ablation experiments // Med. Phys. – 2011. – Vol. 38. – P. 2674–84. doi: 10.1118/1.3570577
12. Davidson S.R.H., Sherar M.D. Measurement of the thermal conductivity of polyacrylamide tissue-equivalent material // Int. J. Hyperthermia. – 2003. – Vol. 19(5). – P. 551-62. doi: 10.1080/0265673031000160799 5
13. Ningrum E.O., Purwanto A., Rosita G.C., Bagus A. The Properties of Thermosensitive Zwitterionic Sulfobetaine NIPAM-co-DMAAPS Polymer and the Hydrogels: The Effects of Monomer Concentration on the Transition Temperature and Its Correlation with the Adsorption Behavior // Indones. J. Chem. – 2020. – Vol. 20 (2). – P. 324-335. doi: 10.22146/ijc.41499
14. Vogel A., Venugopoplan V. Mechanisms of Pulsed Laser Ablation of Biological Tissues // Chem. Rev. – 2003. – Vol. 103. – P. 577–644. doi: 10.1021/cr030683b
15. Minton J.A., Iravani A., Yousefi A. Improving the homogeneity of tissue-mimicking cryogel phantoms for medical imaging // Med. Phys. – 2012. – Vol. 39(11). – P. 6796-807. doi: 10.1118/1.4757617
16. Guntur S.R., Choi M.J. An improved tissue-mimicking polyacrylamide hydrogel phantom for visualizing thermal lesions with high-intensity focused ultrasound // Ultrasound in med. and biol. – 2014. – Vol. 40(11). – P. 2680-2691. doi: 10.1016/j.ultrasmedbio.2014.06.010
17. Welch A.J., Gemert M.J.C. Optical-thermal response of laser-irradiation tissue. // Springer. – 2011. – 947 p. doi:10.1007/978-90-481-8831-4
18. Kang U.K., Папаян Г.В., Березин И.Б., Jin Bae-Soo, Ким С.В., Петрищев Н.Н. Мультиспектральные флуоресцентные органоскопы для прижизненных исследований лабораторных животных и их органов // Оптический журнал. –2011. – Vol. 78(9). – P. 82-90.
19. Korganbayev S., Orrico A., Bianchi L., De Landro M., Wolf A., Dostovalov A., Saccomandi P. Closed-Loop Temperature Control Based on Fiber Bragg Grating Sensors for Laser Ablation of Hepatic Tissue // Sensors 2020. – Vol. 20(22). – P. 6496. doi.org/10.3390/s20226496
20. Manns F., Milne P.J, Gonzalez-Cirre X., Denham, D.B, Parel J., Robinson D.S. In situ temperature measurements with thermocouple probes during laser Interstitial thermotherapy (LITT): quantification and correction of a measurement artifact // Lasers Surg. Med. – 1998. – Vol. 23(2). – P. 94–103. doi: 10.1002/(sici)1096-9101(1998)23:2<94::aid-lsm7>3.0.co;2-q